JACS
JOURNAL OF THE AMERICAN CHEMICAL SOCIETY
Communication
pubs.acs.org/JACS

Hierarchically Porous Polymers from Hyper-cross-linked Block Polymer Precursors

Myungeun Seo,*[,†] Soobin Kim,[†] Jaehoon Oh,[†] Sun-Jung Kim,[‡] and Marc A. Hillmyer[§]

[†]Graduate School of Nanoscience and Technology, Korea Advanced Institute of Science and Technology (KAIST), Daejeon 305-701, Korea

[‡]Mirae Scientific Instruments Inc., Gwangju 500-470, Korea

[§]Department of Chemistry, University of Minnesota, Minneapolis, Minnesota 55455, United States

Supporting Information

ABSTRACT: We report synthesis of hierarchically porous polymers (HPPs) consisting of micropores and well-defined 3D continuous mesopores by combination of hyper-cross-linking and block polymer self-assembly. Copolymerization of 4-vinylbenzyl chloride (VBzCl) with divinylbenzene (DVB) in the presence of polylactide (PLA) macro-chain-transfer agent produced a cross-linked block polymer precursor PLA-*b*-P(VBzCl-*co*-DVB) via reversible addition−fragmentation chain transfer polymerization. A nanoscopic bicontinuous morphology containing PLA and P(VBzCl-*co*-DVB) microdomains was obtained as a result of polymerization-induced microphase separation. While a basic treatment of the precursor selectively removed PLA to yield a reticulated mesoporous polymer, hyper-cross-linking of the precursor by $FeCl_3$ generated micropores in the P(VBzCl-*co*-DVB) microdomain via Friedel−Crafts alkylation and simultaneously degraded PLA to produce the HPP containing micropores in the mesoporous framework. The mesopore size of the HPP could be precisely controlled from 6 to 15 nm by controlling the molar mass of PLA. We demonstrate acceleration in adsorption rate in the HPP compared to a hyper-cross-linked microporous polymer.

Microporous polymers with high surface area are useful for separation, heterogeneous catalysis, and gas storage.[1] A particular interest has been focused on hierarchically porous polymers (HPPs), which contain pores across multiple length scales from micro- (<2 nm) to meso- (2−50 nm) and macropores (>50 nm). While microporous surface provides a main function such as adsorption or catalysis, the existence of mesoporous and macroporous spaces can substantially increase accessibility of the microporous surface by enhanced diffusion, resulting in overall efficiency increase.[2] Such a material should possess an interconnected pore structure to facilitate diffusion, and the pore generation methodologies should provide orthogonal control over pore size and porosity at different length scales. Compared to a large number of hierarchically porous inorganic materials reported so far,[2] relatively a few HPPs have been developed.[3−10] We note that hyper-cross-linking has been used to generate micropores in most cases[4−6] which includes covalent arresting of free volume by bridge formation between aromatic rings via Friedel−Crafts alkylation.[11] The microporous framework constructed by hyper-cross-linking has been incorporated in macropore structures derived from high internal phase emulsion templating,[4] polymerization-induced phase separation,[5] or intersphere cross-linking.[6] However, it has been still challenging to achieve HPPs with micro- and mesopores with explicit mesopore control.

Self-assembly of block polymers consisting of a sacrificial block can produce mesoporous polymers with robust control over pore size.[12] By selectively removing the sacrificial component from a microphase-separated block polymer, a mesoporous polymer with well-defined pore structures such as hexagonally packed cylindrical pores can be obtained and the pore size can be precisely adjusted by molar mass of the sacrificial block. A well-established example of such a block polymer precursor is polystyrene-*block*-polylactide (PS-*b*-PLA), where PLA can be readily etched in basic condition.[13] We recently reported formation of reticulated mesoporous polymers (RMPs) with three-dimensionally (3D) continuous pore structure from a cross-linked bicontinuous PS-*b*-PLA precursor, which was generated by copolymerization of styrene and divinylbenzene (DVB) in the presence of PLA macro-chain-transfer agent (PLA-CTA)[13g] via reversible addition−fragmentation chain-transfer (RAFT) process.[14] Polymerization-induced microphase separation (PIMS) between the PLA and the forming P(S-*co*-DVB) blocks generated a disordered bicontinuous morphology which was arrested by in situ cross-linking. Pore size control from 4 to 8 nm (based on Barrett−Joyner−Halenda (BJH) analysis[15] of nitrogen sorption isotherms) was demonstrated by varying molar mass of PLA. The PIMS process is synthetically feasible and can be applied to other block polymer systems to generate the bicontinuous morphology.[16]

Toward HPPs containing micropores in the 3D continuous mesoporous framework, we combined PIMS process and hyper-cross-linking. Using 4-vinylbenzyl chloride (VBzCl) as a vinyl monomer that can participate in hyper-cross-linking, we followed PIMS protocol to synthesize PLA-*b*-P(VBzCl-*co*-DVB) as a new cross-linked block polymer precursor. While PLA etching of the precursor by basic treatment produced the RMP consistent with our previous study,[13g] hyper-cross-linking

Received: November 11, 2014
Published: December 31, 2014

DOI: 10.1021/ja511581w
J. Am. Chem. Soc. 2015, 137, 600−603

reaction with $FeCl_3$ generated micropores in the P(VBzCl-*co*-DVB) microdomain and also degraded the PLA microdomain to yield the HPP containing micropores in the mesoporous cross-linked PS matrix. The process is schematically illustrated in Figure 1.

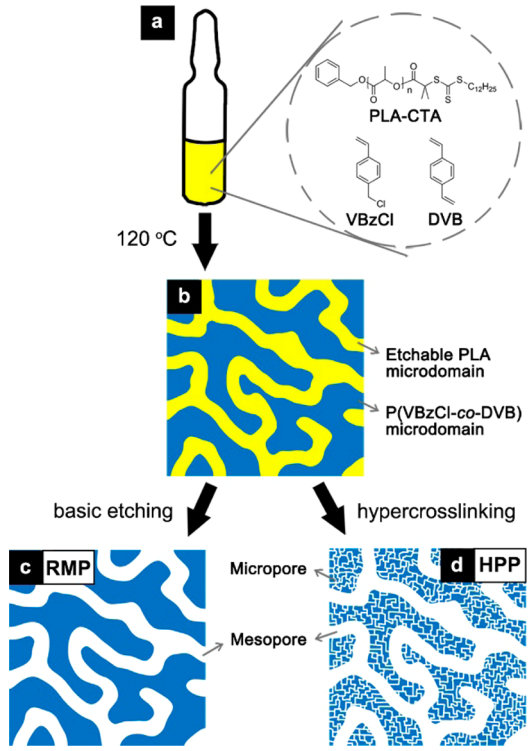

Figure 1. Schematic depiction of RMP and HPP formation. (a) A polymerization mixture containing PLA-CTA, VBzCl, and DVB. (b) PLA-*b*-P(VBzCl-*co*-DVB) is formed via RAFT copolymerization when the mixture is heated to 120 °C, and a nanoscopic bicontinuous morphology consisting of PLA and P(VBzCl-*co*-DVB) microdomains arises as a result of PIMS process. (c) PLA etching of the block polymer precursor under basic condition produces a RMP with 3D continuous pore structure. (d) Addition of $FeCl_3$ to the precursor generates micropores via hyper-cross-linking in the P(VBzCl-*co*-DVB) microdomain and also simultaneously degrades the PLA microdomain, resulting in a HPP with micro- and mesopores.

RAFT polymerization of VBzCl and copolymerization with styrene has been reported previously[17] including use of *S*-1-dodecyl-*S*′-(*R*,*R*′-dimethyl-*R*″-acetic acid) trithiocarbonate-derived macro-CTA.[17c] We coupled hydroxyl-terminated PLAs with *S*-1-dodecyl-*S*′-(*R*,*R*′-dimethyl-*R*″-acetic acid) trithiocarbonate via esterification to form PLA-CTAs,[13c,g] and used them for RAFT copolymerization of VBzCl and DVB. The PLA-CTAs were designated as PLA-CTA-xx, where xx represents the number-average molar mass of the PLA-CTA (kg/mol) (see Supporting Information, Table S1 and Figure S1 for details). Typically, a polymerization mixture containing PLA-CTA (ca. 30 wt%), VBzCl and DVB (4:1 as a molar ratio) was prepared (see Table S2 for the detailed compositions). After degassing, the mixture was heated to 120 °C for 5 h to produce a cross-linked monolith, which was yellow (due to color of the CTA) and transparent. Small angle X-ray scattering (SAXS) analysis of the monoliths showed a broad principal peak (q^*) accompanied by a shoulder at approximately $2q^*$ consistent with a nanoscopic bicontinuous morphology consisting of PLA and P(VBzCl-*co*-DVB) microdomains via PIMS (Figure S2).[13g] From the position of the principal peak, domain spacing (d) of the cross-linked monoliths were determined as 17, 28, and 32 nm when PLA-CTA-11, PLA-CTA-25, and PLA-CTA-41 was used, respectively.

We confirmed that RMPs could be derived from those precursors by PLA etching in 0.5 M NaOH (H_2O/methanol = 6/4) solution at 70 °C for 3 days. A FTIR spectrum of the RMP corroborated complete removal of PLA by disappearance of a vibration frequency at 1749 cm^{-1} corresponding to the carbonyl stretching of PLA (Figure S3). We also note that vibration frequencies at 1264 and 673 cm^{-1} representing C−Cl stretching in benzyl chloride groups were still visible after PLA etching.[18] Elemental analysis data suggest that approximately 40% of the benzyl chloride groups remained intact during the post treatment with the basic etching solution (Table S3). Compared with the precursors, the RMPs showed essentially identical patterns with increased SAXS intensity and slightly reduced d indicating that the microphase-separated structure was successfully retained (Figure S4). The 3D continuous mesopore structure visualized by scanning electron microscopy (SEM) was consistent with the SAXS data (Figure S5). BJH analysis of the desorption branch obtained by nitrogen sorption isotherm experiments gave average pore diameters of 4, 7, and 9 nm when the RMPs were prepared from PLA-CTA-11, PLA-CTA-25, and PLA-CTA-41, respectively (Figure S6 and Table S4).[19] All the data support robust control over mesopore size by molar mass of PLA. Figure 2a,c,e shows SEM, SAXS, and nitrogen sorption isotherm data of the RMP synthesized from PLA-CTA-41 (entry 3, Table S2) as an example.

To produce HPPs, hyper-cross-linking was conducted with the precursors (i.e., PLA-*b*-P(VBzCl-*co*-DVB)s) prior to PLA

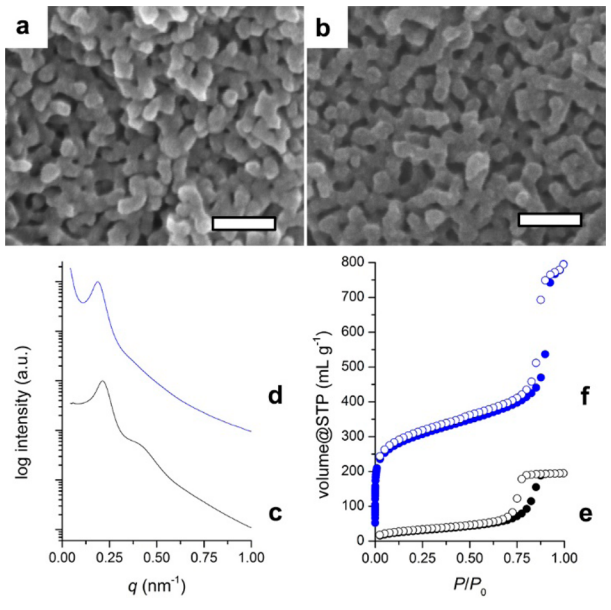

Figure 2. SEM, SAXS, and nitrogen sorption isotherm data of RMP (a,c,e) and HPP (b,d,f) derived from PLA-*b*-P(VBzCl-*co*-DVB) with PLA-CTA-41 (entry 3, Table S2). (a,b) SEM images of the RMP (a) and the HPP (b) taken after Pt coating (1 nm thick). Scale bar represents 100 nm. (c,d) SAXS data of the RMP (c, black) and the HPP (d, blue). The SAXS pattern of the HPP is vertically shifted for clarity. (e,f) Nitrogen sorption isotherm data of the RMP (e, black) and the HPP (f, blue). Filled and empty circles denote adsorption and desorption branches, respectively.

DOI: 10.1021/ja511581w
J. Am. Chem. Soc. 2015, 137, 600−603

etching. Based on a typical hyper-cross-linking procedure,[20] the entire monolith was swollen in 1,2-dichloroethane (a good solvent for both PS and PLA) and then $FeCl_3$ (0.8 eq relative to VBzCl) was added to promote Friedel–Crafts alkylation in the P(VBzCl-*co*-DVB) microdomain and also simultaneously degrade PLA by cleaving ester linkages.[21] Disappearance of the bands at 1749, 1264, and 673 cm^{-1} in the FTIR spectrum was consistent with degradation of PLA and consumption of benzyl chloride moieties by Friedel–Crafts alkylation (Figure S7). However, a vibration band at 1698 cm^{-1} indicated species containing carbonyl groups remained in the material. To ensure removal of any PLA-related residues, we subsequently treated the polymers with NaOH solution.

Figure 2b,d,e represents SEM, SAXS, and nitrogen sorption isotherm data of the HPP synthesized from PLA-CTA-41 so that the data can be directly compared to that of the relevant RMP. SEM imaging revealed percolating mesoporous space equivalent to that in the RMP, but it was not possible to visualize micropores (Figure S8). SAXS data of HPPs were also comparable to those of RMPs, but the shoulder at $2q^*$ was less apparent, suggesting partial loss of long-range order during hyper-cross-linking (Figure S9). Formation of micropores was directly discerned by the nitrogen sorption isotherm which showed apparent uptake at low relative pressure. In case of the HPP synthesized from PLA-CTA-41, pore volume of 0.30 mL/g and surface area of 560 m^2/g were estimated for micropores by t-plot analysis.[22] The isotherm also clearly indicated the existence of mesopores suggesting a HPP with pore volume of 1.19 mL/g and surface area of 940 m^2/g (by Brunauer–Emmett–Teller analysis[23]) was obtained in a single hyper-cross-linking step.

Figure 3 shows nitrogen sorption isotherm data of the HPPs derived from PLA-CTAs with different molar mass of PLA.

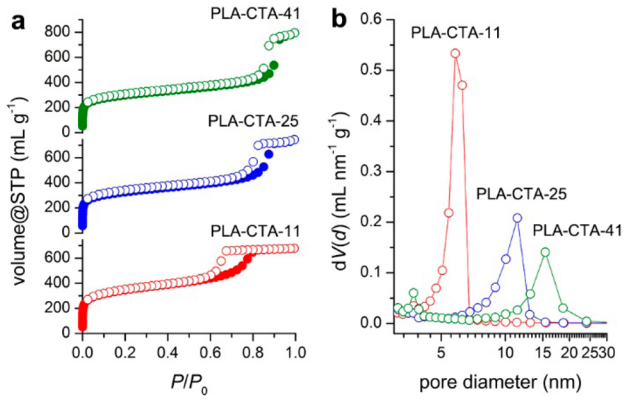

Figure 3. (a) Nitrogen sorption isotherms of HPPs derived from PLA-*b*-P(VBzCl-*co*-DVB)s with different PLA-CTAs. Red: PLA-CTA-11 (entry 1, Table S2). Blue: PLA-CTA-25 (entry 2, Table S2). Green: PLA-CTA-41 (entry 3, Table S2) [same data as in Figure 2f]. Filled circles: adsorption. Empty circles: desorption. (b) Mesopore size distributions based on BJH analysis of the desorption branches.

HPPs typically exhibited pore volume of ~1 mL/g and surface area of ~1000 m^2/g (detailed pore characteristics are summarized in Table S5). Precise control over mesopore size by molar mass of PLA could be achieved from 6 to 15 nm based on BJH analysis, giving a distinct advantage to this methodology over intersphere cross-linking method.[6d] We note that size of the mesopores in the HPPs was larger than those in the RMPs (for example, 15 vs 9 nm in case of PLA-CTA-41) presumably because hyper-cross-linking in the swollen state would increase the domain spacing (see Figure S10) and shrink the P(VBzCl-*co*-DVB) microdomain. While size of the micropores formed by hyper-cross-linking appears to vary little, we expect pore volume and surface area occupied by micropores and mesopores can be adjusted by varying ratio of PLA-CTA, VBzCl, and DVB in the polymerization mixture. To illustrate this point, we synthesized a HPP from a mixture containing PLA-CTA-41 (28 wt%), VBzCl, and DVB (1:1 molar ratio) and found pore volume and surface area increased to 1.63 mL/g and 1180 m^2/g, compared with 1.19 mL/g and 940 m^2/g obtained from a mixture of PLA-CTA-41 (27 wt%), VBzCl, and DVB (4:1 molar ratio) (Figure S11).

To demonstrate improvement in adsorption rate by the existence of the 3D continuous mesoporous space, we measured nitrogen adsorption kinetics of a HPP synthesized from PLA-CTA-27 (mesopore size 10 nm) and compared the data with those of a microporous polymer synthesized by hyper-cross-linking (see Figure S12 for their nitrogen sorption isotherms). The microporous polymer was obtained by reacting $FeCl_3$ with P(VBzCl-*co*-DVB), which was synthesized by RAFT copolymerization of VBzCl and DVB in the presence of a molecular CTA (i.e., without PLA). Figure 4 shows change in

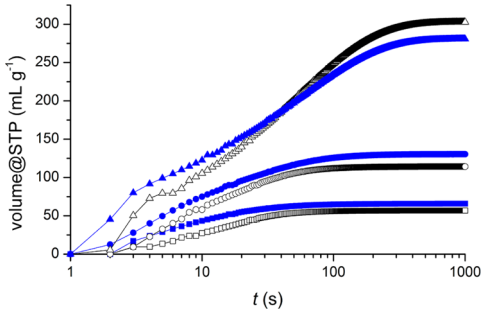

Figure 4. Nitrogen adsorption kinetics for a microporous polymer (black) and a HPP (blue) when different pressure was applied. Squares, circles, and triangles denote initial pressure of 6.7, 13.3, and 40.0 kPa, respectively.

the amount of adsorbed nitrogen as a function of time at different applied pressures (see Figure S13 for the system configuration). At given pressure, the nitrogen uptake rapidly increased initially and was plateaued when the system reached equilibrium. Calculating the exact rate of adsorption was difficult because both adsorption and dead volume filling contributed to the nitrogen uptake in the early stage (Figure S14). However, in any case it was apparent that nitrogen was always adsorbed more rapidly in the HPP than the microporous polymer in the early stage of the measurement. This initial study supports accelerated adsorption by enhanced diffusion through the mesopores.

In summary, we have developed a facile synthetic route for HPPs containing micropores within the mesoporous framework by combination of block polymer self-assembly and hyper-cross-linking. We expect this HPP will prove useful where rapid sorption kinetics through well-defined 3D continuous mesoporous space is important.

DOI: 10.1021/ja511581w
J. Am. Chem. Soc. 2015, 137, 600–603

■ ASSOCIATED CONTENT

Supporting Information

Synthetic details, Figures S1−S14, and Tables S1−S5. This material is available free of charge via the Internet at http://pubs.acs.org.

■ AUTHOR INFORMATION

Corresponding Author

seomyungeun@kaist.ac.kr

Notes

The authors declare no competing financial interest.

■ ACKNOWLEDGMENTS

The authors thank Prof. Gon Seo, Morgan Schulze, and Stacey Saba for helpful input. This research was supported by Basic Science Research Program through the National Research Foundation of Korea (NRF) funded by the Ministry of Education, Science and Technology (NRF-2014-R1A1A1004941), and also by Dow Chemical Co. and the National Science Foundation (DMR-1006370). Parts of this work were carried out in the College of Science and Engineering Characterization Facility, University of Minnesota, a member of the NSF-funded Materials Research Facilities Network. SAXS data were acquired by members of the DuPont-Northwestern-Dow Collaborative Access Team (DND-CAT), located at Sector 5 of the Advanced Photon Source (APS). DND-CAT is supported by E.I. DuPont de Nemours & Co., The Dow Chemical Co., and Northwestern University. Use of the APS, an Office of Science User Facility operated for the U.S. Department of Energy (DOE) Office of Science by Argonne National Laboratory, was supported by the U.S. DOE under Contract No. DE-AC02-06CH11357.

■ REFERENCES

(1) (a) Wu, D.; Xu, F.; Sun, B.; Fu, R.; He, H.; Matyjaszewski, K. *Chem. Rev.* **2012**, *112*, 3959−4015. (b) Dawson, R.; Cooper, A. I.; Adams, D. J. *Prog. Polym. Sci.* **2012**, *37*, 530−563.

(2) *Hierarchically Structured Porous Materials*; Su, B.-L., Sanchez, C., Yang, X.-Y., Eds.; Wiley: Weinheim, 2012.

(3) (a) Wong, L. L. C.; Ikem, V. O.; Menner, A.; Bismarck, A. *Macromol. Rapid Commun.* **2011**, *32*, 1563−1568. (b) Wong, L. L. C.; Villafranca, P. M. B.; Menner, A.; Bismarck, A. *Langmuir* **2013**, *29*, 5952−5961. (c) Pulko, I.; Krajnc, P. *Macromol. Rapid Commun.* **2012**, *33*, 1731−1746. (d) Sušec, M.; Ligon, S.; Stampfl, J.; Liska, R.; Krajnc, P. *Macromol. Rapid Commun.* **2013**, *34*, 938−943. (e) Sevšek, U.; Brus, J.; Jeřabek, K.; Krajnc, P. *Polymer* **2014**, *55*, 410−415. (f) Ma, L.; Luo, X.; Cai, N.; Xue, Y.; Zhu, S.; Fu, Z.; Yu, F. *Appl. Surf. Sci.* **2014**, *305*, 186−193.

(4) (a) Schwab, M. G.; Senkovska, I.; Rose, M.; Klein, N.; Koch, M.; Pahnke, J.; Jonschker, G.; Schmitz, B.; Hirscher, M.; Kaskel, S. *Soft Matter* **2009**, *5*, 1055−1059. (b) Pulko, I.; Wall, J.; Krajnc, P.; Cameron, N. R. *Chem.—Eur. J.* **2010**, *16*, 2350−2354.

(5) (a) Oh, C.-G.; Ahn, J.-H.; Ihm, S.-K. *React. Funct. Polym.* **2003**, *57*, 103−111. (b) Xie, Z. *Mater. Lett.* **2009**, *63*, 509−511. (c) Urban, J.; Svec, F.; Fréchet, J. M. J. *Anal. Chem.* **2010**, *82*, 1621−1623. (d) Urban, J.; Svec, F.; Fréchet, J. M. J. *J. Chromatogr. A* **2010**, *1217*, 8212−8221. (e) Maya, F.; Svec, F. *Polymer* **2014**, *55*, 340−346.

(6) (a) Zeng, Q.; Wu, D.; Zou, C.; Xu, F.; Fu, R.; Li, Z.; Liang, Y.; Su, D. *Chem. Commun.* **2010**, *46*, 5927−5929. (b) Zou, C.; Wu, D.; Li, M.; Zeng, Q.; Xu, F.; Huang, Z.; Fu, R. *J. Mater. Chem.* **2010**, *20*, 731−735. (c) Lee, D.; Zhang, C.; Wei, C.; Ashfeld, B. L.; Gao, H. *J. Mater. Chem. A* **2013**, *1*, 14862−14867. (d) Li, Z.; Wu, D.; Huang, X.; Ma, J.; Liu, H.; Liang, Y.; Fu, R.; Matyjaszewski, K. *Energy Environ. Sci.* **2014**, *7*, 3006−3012.

(7) (a) Wang, J.; Lessard, B. H.; Maric, M.; Favis, B. D. *Polymer* **2014**, *55*, 3461−3467. (b) Gao, J.; Wong, J. S.-P.; Hu, M.; Li, W.; Li, R. K. Y. *Nanoscale* **2014**, *6*, 1056−1063.

(8) (a) Rose, M.; Klein, N.; Senkovska, I.; Schrage, C.; Wollmann, P.; Böhlmann, W.; Böhringer, B.; Fichtner, S.; Kaskel, S. *J. Mater. Chem.* **2011**, *21*, 711−716. (b) Wilke, A.; Weber, J. *J. Mater. Chem.* **2011**, *21*, 5226−5229. (c) Wang, J.; Xu, S.; Wang, Y.; Cai, R.; Lu, C.; Qiao, W.; Long, D.; Ling, L. *RSC Adv.* **2014**, *4*, 16224−16232.

(9) Valkama, S.; Nykänen, A.; Kosonen, H.; Ramani, R.; Tuomisto, F.; Engelhardt, P.; ten Brinke, G.; Ikkala, O.; Ruokolainen, J. *Adv. Funct. Mater.* **2007**, *17*, 183−190.

(10) (a) Sai, H.; Tan, K.; Hur, K.; Asenath-Smith, E.; Hovden, R.; Jiang, Y.; Riccio, M.; Muller, D. A.; Elser, V.; Estroff, L. A.; Gruner, S. M.; Wiesner, U. *Science* **2013**, *341*, 530−534. (b) Dorin, R. M.; Sai, H.; Wiesner, U. *Chem. Mater.* **2014**, *26*, 339−347.

(11) For reviews, see: (a) Tsyurupa, M. P.; Davankov, V. A. *React. Funct. Polym.* **2006**, *66*, 768−779. (b) Zhang, X.; Shen, S.; Fan, L. *J. Mater. Sci.* **2007**, *42*, 7621−7629. (c) Xu, S.; Luo, Y.; Tan, B. *Macromol. Rapid Commun.* **2013**, *34*, 471−484.

(12) Olson, D. A.; Chen, L.; Hillmyer, M. A. *Chem. Mater.* **2008**, *20*, 869−890.

(13) (a) Zalusky, A. S.; Olayo-Valles, R.; Taylor, C. J.; Hillmyer, M. A. *J. Am. Chem. Soc.* **2001**, *123*, 1519−1520. (b) Zalusky, A. S.; Olayo-Valles, R.; Wolf, J. H.; Hillmyer, M. A. *J. Am. Chem. Soc.* **2002**, *124*, 12761−12773. (c) Rzayev, J.; Hillmyer, M. A. *J. Am. Chem. Soc.* **2005**, *127*, 13373−13379. (d) Mao, H.; Hillmyer, M. A. *Soft Matter* **2006**, *2*, 57−59. (e) Chen, L.; Hillmyer, M. A. *Macromolecules* **2009**, *42*, 4237−4243. (f) Seo, M.; Amendt, M. A.; Hillmyer, M. A. *Macromolecules* **2011**, *44*, 9310−9318. (g) Seo, M.; Hillmyer, M. A. *Science* **2012**, *336*, 1422−1425. (h) Seo, M.; Murphy, C. J.; Hillmyer, M. A. *ACS Macro Lett.* **2013**, *2*, 617−620.

(14) (a) Moad, G.; Rizzardo, E.; Thang, S. H. *Aust. J. Chem.* **2006**, *59*, 669−692. (b) Moad, G.; Rizzardo, E.; Thang, S. H. *Aust. J. Chem.* **2009**, *62*, 1402−1472. (c) Moad, G.; Rizzardo, E.; Thang, S. H. *Aust. J. Chem.* **2012**, *65*, 1402−1472. (d) Monteiro, M. J. *J. Polym. Sci., Part A: Polym. Chem.* **2005**, *43*, 3189−3204. (e) Barner, L.; Davis, T. P.; Stenzel, M.; Barner-Kowollik, C. *Macromol. Rapid Commun.* **2007**, *28*, 539−559.

(15) Barrett, E. P.; Joyner, L. G.; Halenda, P. P. *J. Am. Chem. Soc.* **1951**, *73*, 373−380.

(16) Schulze, M. W.; McIntosh, L. D.; Hillmyer, M. A.; Lodge, T. P. *Nano Lett.* **2014**, *14*, 122−126.

(17) (a) Chen, Y.; Chen, G.; Stenzel, M. H. *Macromolecules* **2010**, *43*, 8109−8114. (b) Manguian, M.; Save, M.; Chassenieux, C.; Charleux, B. *Colloid Polym. Sci.* **2005**, *284*, 142−150. (c) Gu, Y.; Zhang, S.; Martinetti, L.; Lee, K. H.; McIntosh, L. D.; Frisbie, C. D.; Lodge, T. P. *J. Am. Chem. Soc.* **2013**, *135*, 9652−9655. (d) Moraes, J.; Ohno, K.; Gody, G.; Maschmeyer, T.; Perrier, S. *Beilstein J. Org. Chem.* **2013**, *9*, 1226−1234.

(18) Meng, G.; Li, A.; Yang, W.; Liu, F.; Yang, X.; Zhang, Q. *Eur. Polym. J.* **2007**, *43*, 2732−2737.

(19) The BJH pore diameter may not represent the exact pore size of the present mesoporous network as the analysis assumes 1D cylindrical pores. However we believe that it still provides a meaningful and standard value that can be compared to other porous materials.

(20) (a) Ahn, J.-H.; Jang, J.-E.; Oh, C.-G.; Ihm, S.-K.; Cortez, J.; Sherrington, D. C. *Macromolecules* **2006**, *39*, 627−632. (b) Germain, J.; Hradil, J.; Fréchet, J. M. J.; Svec, F. *Chem. Mater.* **2006**, *18*, 4430−4435. (c) Liu, Q. *Macromol. Chem. Phys.* **2010**, *211*, 1012−1017.

(21) Lian, X.; Fu, S.; Ma, T.; Li, S.; Zeng, W. *Appl. Organomet. Chem.* **2011**, *25*, 443−447.

(22) Lowell, S.; Shields, J. E.; Thomas, M. A.; Thommes, M. *Characterization of Porous Solids and Powders: Surface Area, Pore Size and Density*; Kluwer Academic Publishers: Amsterdam, 2004; Chapter 9.2.2.

(23) Brunauer, S.; Emmett, P. H.; Teller, E. *J. Am. Chem. Soc.* **1938**, *60*, 309−319.

DOI: 10.1021/ja511581w
J. Am. Chem. Soc. 2015, 137, 600−603